11th Canadian Masonry Symposium, Toronto, Ontario, May 31- June 3, 2009

OUT-OF-PLANE SEISMIC BEHAVIOUR OF BRICK MASONRY INFILLED PANELS WITH PRIOR IN-PLANE DAMAGE

Durgesh C. Rai[1], S. Komaraneni[2] and Vaibhav Singhal[3]

[1] Associate Professor, Department of Civil Engineering, Indian Institute of Technology Kanpur, Kanpur, UP 208016, India, dcrai@iitk.ac.in

[2] Graduate Student, Department of Civil Engineering, Indian Institute of Technology Kanpur, Kanpur, UP 208016, India, komaraneni1984@gmail.com

[3] Ph.D. Student, Department of Civil Engineering, Indian Institute of Technology Kanpur, Kanpur, UP 208016, India, singhal@iitk.ac.in

ABSTRACT

Half-scaled clay brick infill masonry panels were subjected to a sequence of slow cyclic in-plane drifts and shake table generated out-of-plane ground motions to assess the interaction of in-plane damage over the out-of-plane behaviour. The results show that the infill panels maintained structural integrity and out-of-plane stability even when severely damaged; and out-of-plane failure may not be because of excessive inertial forces only but can be due to large out-of-plane deflections. Also, the weaker interior grid elements which divide the masonry in smaller sub-panels were able to delay the failure by controlling out-of-plane deflection and significantly enhancing in-plane response.

KEYWORDS: Masonry, infills, stability, seismic response.

INTRODUCTION

In general, the masonry infills are subjected to in-plane as well as out-of-plane loads simultaneously during an earthquake. Their load carrying capacity in out-of-plane direction after being damaged in in-plane direction is crucial. Furthermore, it is always possible to have aftershocks after a major earthquake, which can dislodge these already cracked and loosened infills due to inertial forces normal to its plane. The out-of-plane strength may be substantially weakened by in-plane cracking of the panels. Consequently, out-of-plane strength of cracked infills is often assumed to be negligibly low and is neglected in the seismic evaluation process and, therefore, usual mitigation measures consisting of either replacement of infills or their strengthening may not be necessary.

All the previous research on out-of-plane behaviour of masonry panel have considered the important factors, like slenderness ratio, panel thickness, boundary conditions, overburden pressure, etc., that affect the out-of-plane strength. However, relatively not much work has been done on the effect of in-plane damage on the out-of-plane behaviour, which is the most important

factor to be considered to actually predict the behaviour of masonry during earthquakes. Research studies by Angel et al. (1994) [1] and Flanagan and Benette (1999) [2] have considered this effect by applying known damage to the specimen before exposing it to out-of-plane loading. The two studies have applied the out-of-plane loading as a slow incremental uniform pressure using an air bag. Angel et al. (1994) have considered the single in-plane damage magnitude as two times of the lateral drift corresponding to initial cracking, while Flanagan and Benette (1999) have considered the drift corresponding to 80% of the in-plane load capacity of the controlled specimen. It is not possible to predict the level of in-plane damage that the masonry infills will undergo during an earthquake; hence, it is clear that the out-of-plane strength of masonry at a single in-plane damage level is not adequate to predict its post cracking behaviour. Also, during the ground motion the cracks opened in the specimen are automatically closed when the direction of motion changes, which may result in more stable condition than the monotonically increasing uniform air bag pressure.

The present study is an extension of the research in this area by considering the dynamic out-of-plane loading for a cracked infill at different in-plane damage levels. This paper describes preliminary results of an experimental research undertaken to study the behaviour of masonry infill panels under simulated out-of-plane ground motion with prior in-plane damage.

SPECIMEN DETAILS

The experimental work was carried out on two half-scaled wall specimens as shown in Figure 1. The prototype wall considered is a ½-brick thick wall of dimensions 5 m×3 m. Therefore, for the 1:2 scaled specimen, the dimensions will be 2.5 m×1.5 m and 60 mm thick, such that slenderness ratio, h/t = 23. The specimens were provided with weak moment resisting frames made of confining grid elements of 60 mm×40 mm cross section. The top beam of this frame was made 100 mm thick to maintain the better grip of load transferring mechanism with the actuator.

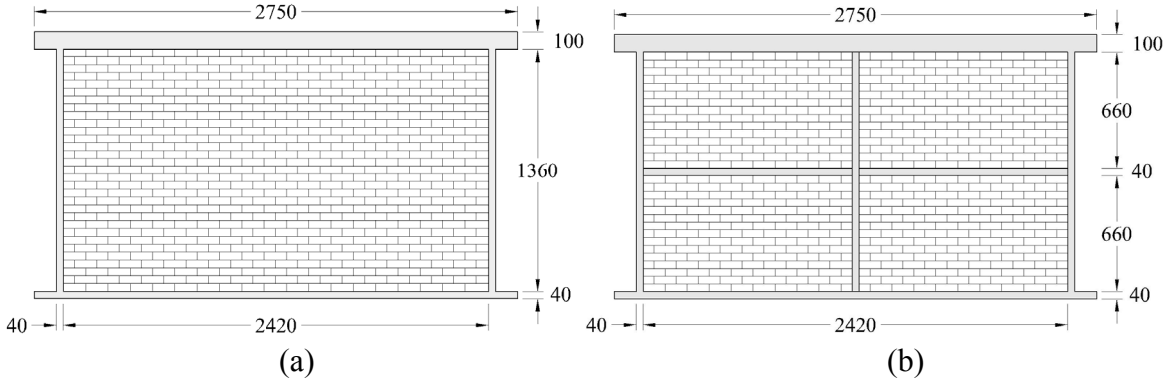

Figure 1: Geometric details of (a) Specimen 1 (b) Specimen 2

MATERIAL PROPERTIES

The micro-concrete of mix proportion 0.50:1:2.75 (water: cement: aggregate) of 25 MPa as characteristic compressive strength was used in all the member of confining frame. The target cube compressive strength of design mix at 28-days was found to be 30.6 MPa. Specially made half-scaled burnt clay bricks (120.2×59.5×36.6 mm) and lime cement mortar of mix proportion 1:1:6 (cement: lime: sand) was used. The average compressive strength of the brick and mortar was found as 46.04 MPa and 4.91 MPa, respectively.

Five-brick thick masonry prisms were made at the time of laying the brick wall and were moist cured for 28-days before testing. The average compressive strength and modulus of elasticity of masonry prism was found out to be 6.62 MPa and 3412 MPa, respectively. To measure the shear strength of the masonry, diagonal tension tests according to ASTM E 519-07 [3] were carried out on 0.6 m×0.6 m size specimens using half-scaled bricks. The average shear stress of masonry at 28-days was found as 0.2 MPa.

ARTIFICIAL MASS SIMULATION

For a reliable correlation study with the prototype one of the most important consideration is the appropriate modelling as per similitude relations. Simulation of forces includes both gravitational and inertial types, which can be achieved by adding structurally ineffective lumped masses (Mills et al. 1979) [4]. For the considered half-scaled model bricks, the additional weight to be added is equal to mass of that brick, which is approximately 0.435 kg. Lead blocks of an average mass of 0.865 kg were attached to account for mass of two bricks and they were fixed in regular grid pattern on both face of the wall.

TEST SETUP

Test setup for the present work was prepared in such a way that there is no need to displace the specimen for the repeated cycles of in-plane and out-of-plane loads. The test setup for the out-of-plane loading and in-plane loading are shown in Figures 2. The dead load of 0.10 MPa was maintained over the wall specimen with the help of flexible wire rope arrangement (Figure 2). The uni-axial shake table used for the out-of-plane testing has the dimensions of 1.8 m×1.2 m (length×width) with 1.8 m length in the direction of motion. The 100 kN capacity actuator was used for in-plane loading and four bars of 20 mm diameter were used to connect the both ends of the top beam with the actuator. A sufficient number of supports were provided in-plane and out-of-plane direction to simulate the desired boundary conditions. The lateral supports for the specimen as shown in Figure 2 serve two purposes: they will act as support condition during out-of-plane loading and serves as to restrain any lateral out-of-plane movement during in-plane loading. The in-plane supports are meant for transferring the overturning loads generated during the in-plane loading, without overstressing the table bearings.

For out-of-plane tests, sixteen accelerometers were used: fifteen were attached to the wall and one was fixed to the shake table. Four load cells were kept to measure the variation of vertical compressive load during testing. Four horizontal LVDTs were used to measure the displacements in out-of-plane and in-plane direction, and two LVDTs were used to measure the diagonal contraction and elongation during in-plane loading. A high performance data acquisition system was used to collect data from sensors at a rate of 1 kS/s.

LOADING HISTORY

In the out-of-plane direction, the specimens were subjected to simulated earthquake ground motion generated by a shake table. The out-of-plane target ground motion was chosen as N21E component of the 1952 Taft earthquake with PGA of 0.156*g* and total duration of 54.16 s (Figure 3a). The first 30 s of ground motion was considered for simulation, which includes the strong motion portion, and the time axis of the accelerogram was scaled by a factor $1/\sqrt{2}$ to satisfy the similitude relations.

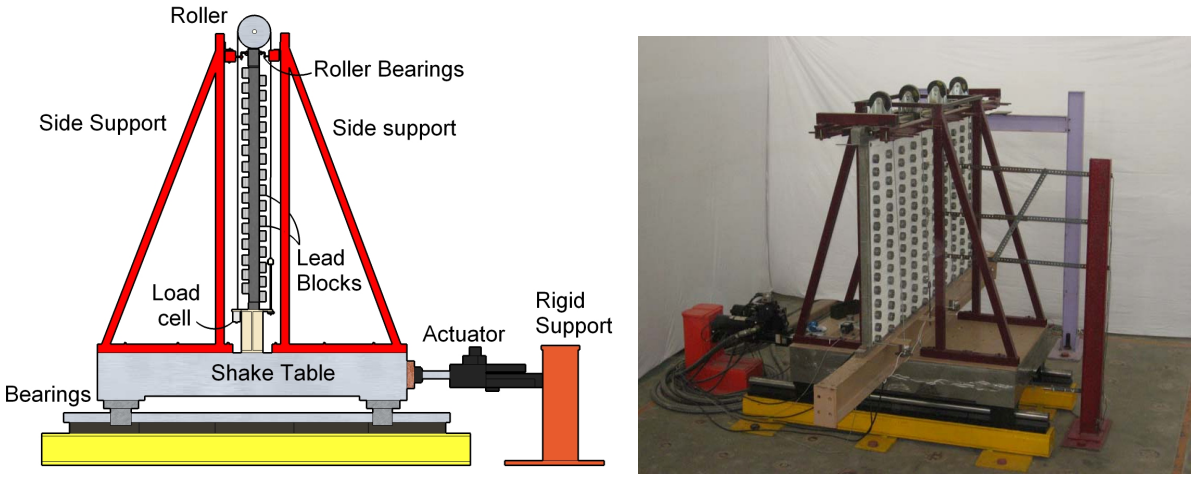

(a)

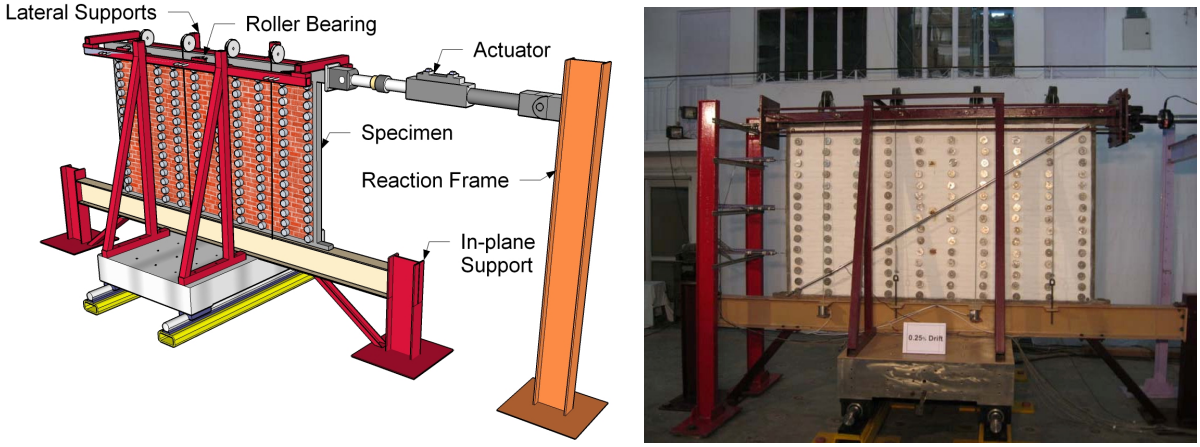

(b)

Figure 2: Test setup for (a) out-of-plane loading and (b) in-plane loading

Response spectra of Taft ground motion was compared with the design response spectra of IS 1893 (BIS 2002) [5] for a design basis earthquake (DBE) in Zone V (PGA = 0.36*g*), and a reasonable match was observed when Taft motion was scaled to make its PGA equal to 0.40*g* as shown in Figure 3b. Taft 0.40*g* ground motion for the Zone-V DBE is referred as Level-V motion. Similarly, the Taft motion scaled to PGA of 0.111*g*, 0.177*g* and 0.266*g* were respectively referred as Level-II, III and IV motions, which correspond to Zone II (0.10*g*), III (0.16*g*) and IV (0.24*g*) of IS 1893-2002. A White noise test of low intensity (0.05*g*) was also conducted to investigate the change in stiffness properties of the specimen after each cycle of Taft earthquake motion.

In-plane loading consists of displacement controlled slow cycle as per ACI 374.1-05 [6]. This loading history consists of gradually increased storey drifts (displacements) of 0.20 %, 0.25 %, 0.35 %, 0.50 %, 0.75 %, 1.00 %, 1.40 %, 1.75 %, and 2.20 %. Each displacement cycle was repeated for three times at each drift ratio.

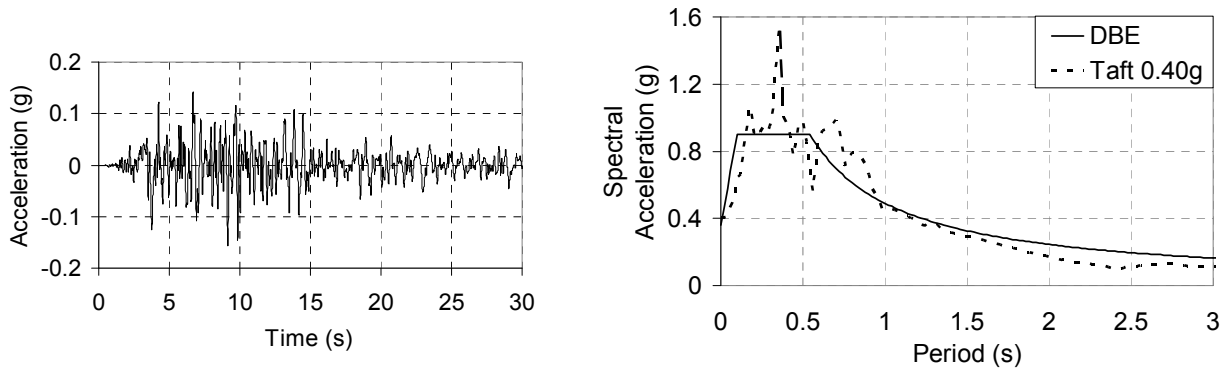

(b) (b)

Figure 3: (a) TAFT N21E ground motion (b) Comparison of response spectra of DBE and TAFT motion

TEST PROCEDURE

After safely mounting the specimen on the shake table, forced vibration tests were carried out on the specimen before the final testing. The test started with out-of-plane shake table motions consisting of series of incremental Taft motions from Level-I to Level-V with White Noise in between them. After the completion of this out-of-plane cycle, the specimen was subjected to slow in-plane cyclic loading. The in-plane cyclic loading was continued until cracks were visible on the specimen and it was observed at 0.50 % drift ratio for the first specimen. The in-plane load was stopped after this drift level and the second cycle of out-of-plane loading was applied. The second cycle of out-of-plane loading consisted of only Level-V Taft motion with White Noise before and after the application of Level-V motion. The second cycle of in-plane loading was with the next level of drift ratio (0.75 %) except for the first specimen. In the first specimen, this was stepped to 1.00 % due to an error in the controller. Again, out-of-plane loading was carried out and the alternate process of in-plane and out-of-plane loading was continued till failure of the specimen as shown in Figure 4. The visual observations were noted down after each cycle of testing and the cracks in the specimen were marked.

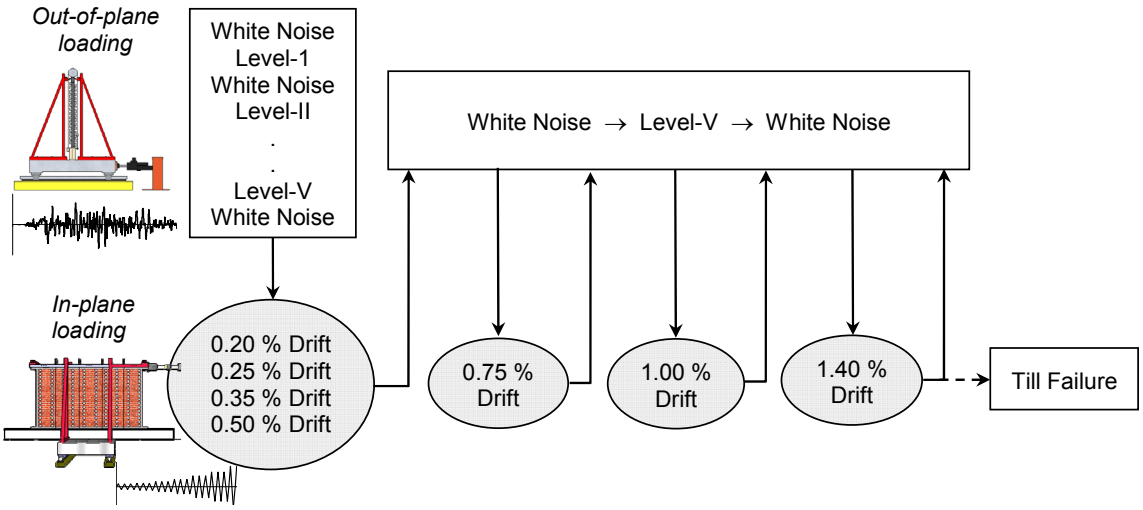

Figure 4: Loading sequence

OBSERVED BEHAVIOUR

Majority of the cracks were formed due to the in-plane loading; only very few cracks were observed during the out-of-plane loading. The cracks formed at initial stages of the in-plane loading widened, and energy dissipation was mainly due to sliding along bed-joints. The first specimen shows a diagonal bed joint cracking pattern, whereas the second specimen showed a sliding along the parallel bed joints and uniformly distributed cracks (Figure 5 and 6). The first and second specimens reached their peak in-plane strengths of 32.2 kN and 39.1 kN at 7.50 mm and 11.25 mm displacements, respectively.

The first specimen collapsed during out-of-plane loading following 1.20 % in-plane drift cycles and showed large out-of-plane deflection and arching before the failure (Figure 5b). However, for the second specimen with interior grid elements, a partial collapse of masonry sub-panels was observed after 2.20 % in-plane drift cycles, along with failure of interior vertical grid element at mid-height (Figure 6b).

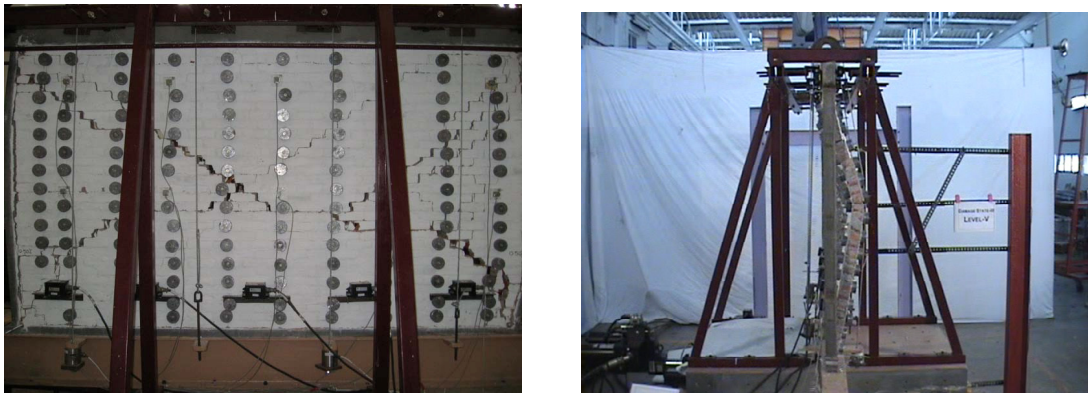

Figure 5: Cracking pattern in the first specimen after 1.0 % in-plane drift cycles and arching phenomenon before failure under out-of-plane shake table motion

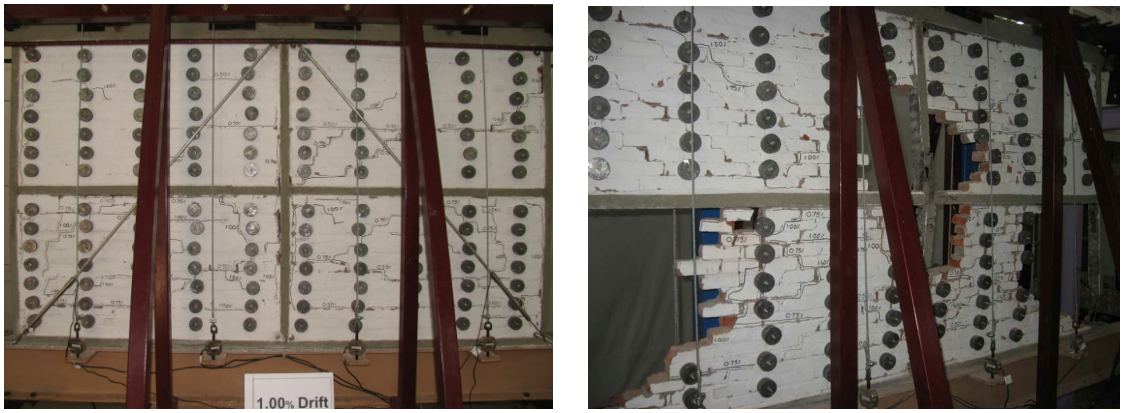

Figure 6: Cracking pattern in the second specimen after 1.0 % in-plane drift cycles and partial collapse of masonry due to out-of-plane motion after 2.2 %in-plane drift cycles

RESULTS AND DISCUSSIONS

Both specimens reached peak accelerations in the undamaged state and once the damage was introduced, the acceleration response decreased and was observed to saturate to a lower value with continued in-plane damage (Figure 7). Slight increase in average acceleration was observed in first specimen after the first in-plane damage state due to the change in the roller arrangement, which increased the vertical compression from the previous arrangement. On the contrary, the out-of-plane deflection continued to increase for the same level of base acceleration input with in-plane damage. This indicates that the observed out-of-plane failure was primarily due to instability caused by excessive deflections, not so much due to increased accelerations (inertia forces), which is also supported by the arching theory.

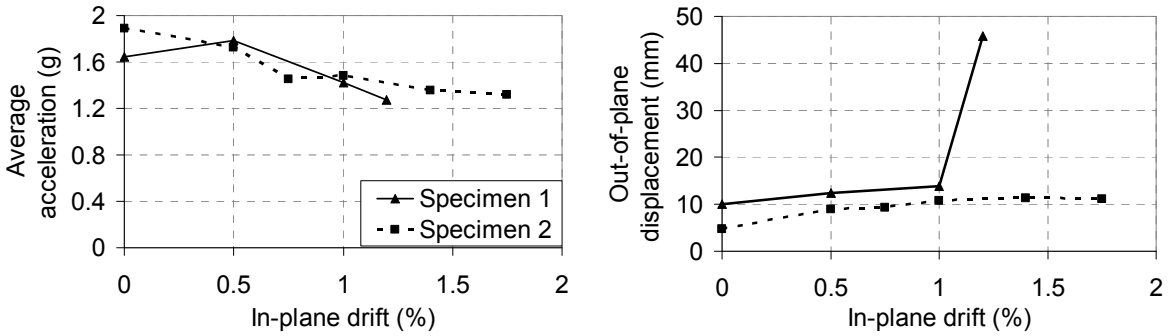

Figure 7: Variation of average acceleration and out-of-plane displacement with in-plane drift (Damage)

Peak acceleration values in both specimens were almost same; however, relatively small deflection was observed for the second specimen (Figure 7). This may be because of the confining effect that the interior grid elements generated, which helped in reducing out-of-plane deflections. The variation of average acceleration along the height of specimens follows nearly same profile for both specimens at various damage levels as shown in Figure 8. With increase in in-plane damage level, acceleration at the top of specimens reduced significantly as compared to the mid-height accelerations and approached to the table acceleration values.

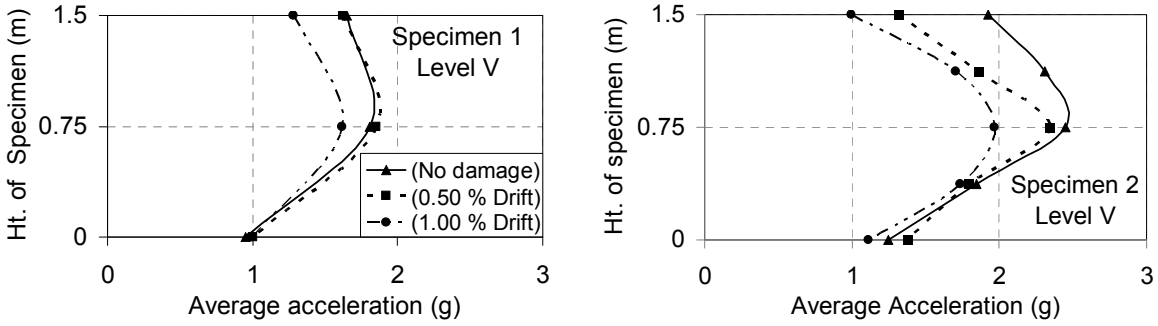

Figure 8: Variation of average accelerations along the height of specimen

The interior grid elements provided in the second specimen appeared not very effective in modifying the acceleration response as its peak values and profile was nearly similar to those of

the first specimen without interior grid elements. This may be due to the poor flexural/torsional resistance provided by the weak grid elements and their flexible connections with the peripheral elements. However, they were quite effective in reducing the out-of-plane deflections, and hence delaying the out-of-plane failure by dislodgement.

The fundamental natural frequencies obtained for both specimens have shown a continuous drop after each in-plane damage state, which indicate the softening of the specimens due to damage (Figure 9). The undamaged specimens have initial fundamental natural frequencies of 9.18 Hz and 10.02 Hz for the first and the second specimen, respectively. The slight increase in natural frequency of the second specimen may be because of increase in stiffness due to the interior grid elements. The total reduction in the frequencies before failure is 25.49 % and 41.06 % for the first and the second specimen, respectively. For the first specimen decrease in natural frequency in the last cycle before failure was higher than the average rate of decrease that it had during the test. In contrast, the second specimen had nearly uniform rate of decrease during the test.

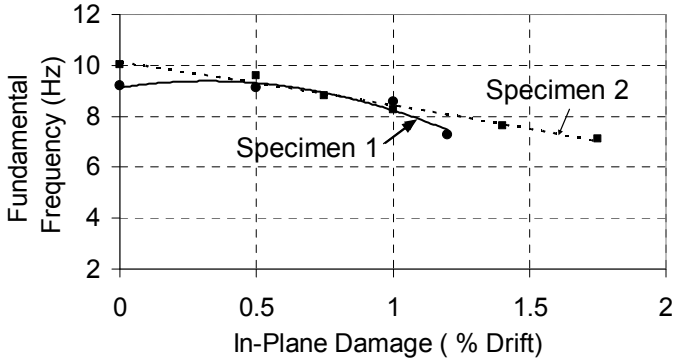

Figure 9: Variation in fundamental frequencies of the specimens.

The in-plane load-displacement response showed enhanced capacity of infill panel with interior grid elements (Figure 10). The sliding motion of sub-panels along the grid elements allowed grater deformability and dissipation of energy without much reduction in lateral resistance. Similar behaviour of masonry with interior grid elements under in-plane loads was observed in an earlier study by Paikara (2005) [7].

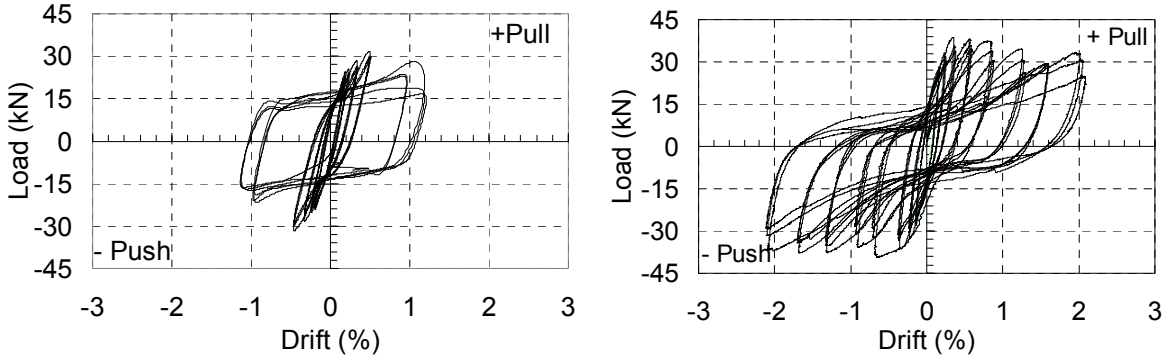

Figure 10: Load-displacement curve (a) Specimen 1 (b) Specimen 2

CONCLUSIONS

The study was concerned with evaluation of out-of-plane response of slender masonry infill panels when damaged due to in-plane forces. Two half-scaled specimens of large slenderness ratio (h/t = 23) were observed to maintain structural integrity and out-of-plane stability under the design level out-of-plane inertial forces even in the damaged state due to in-plane drifts in the excess of 1%. Interior grid elements, which divide the masonry in smaller sub-panels have clearly improved both in-plane as well as out-of-plane response. These not only helped to reduce out-of-plane deflection but also greatly improved the in-plane response and energy dissipation potential and consequently, the out-of-plane failure of masonry was delayed and it could safely sustain large in-plane drifts upto 2.2%. Further, out-of-plane failure of masonry infill panels was not entirely due the accelerations (inertial forces), but adversely affected by excessive out-of-plane displacements, as also suggested by the arching theory. These preliminary observations suggest that the current code approaches to prevent out-of-plane failure of masonry infills are rather conservative and even slender masonry walls have considerable resistance against out-of-plane forces; however, it needs to be further substantiated.

ACKNOWLEDGEMENTS

The financial support provided by the Ministry of Human Resource Development, Government of India in carrying out this experimental research work is gratefully acknowledged.

REFERENCES

1. Angel, R., Abrams, D. P., Shapiro, D., Uzarski, J., and Webster, M. (1994) "Behaviour of reinforced concrete frames with masonry infills" Struct. Res. Ser. 589*,* Department of Civil Engineering, University of Illinois, Urbana-Champaign.
2. Flanagan, R. D., and Bennett, R. M. (1999) "Bidirectional behaviour of structural clay tile infilled frames" Journal of Structural Engineering, ASCE, March 1999.
3. ASTM E 519 (2007) "Standard test method for diagonal tension (shear) in masonry assemblages" Masonry Test Methods and Specification for the Building Industry, American Society for Testing and Materials, Pennsylvania.
4. Mills, R.S., Krawinkler, H., and Gere, J.M. (1979) "Model tests on earthquake simulators-development and implementation of experimental procedures" The John A. Blume Earthquake Engineering Center Report No.39, Stanford University, California, June 1979.
5. BIS: 1893 (2002) "Indian Standard Criteria for Earthquake Resistant Design of Structure, Part 1: General provisions and buildings" Fifth revision, Bureau of Indian Standards, New Delhi, India
6. ACI committee 374 (2006) "Acceptance Criteria for Moment Frames Based on Structural Testing and Commentary" ACI 374.1-05, American Concrete Institute, Farmington Hills, Mich., 6pp.
7. Paikara, S. (2005) "In-plane lateral resistance of masonry confined by grid elements" Thesis report submitted to Dept. of Civil Engg., IIT Kanpur.